Carbohydrate Polymers 102 (2014) 431–437

Contents lists available at ScienceDirect

Carbohydrate Polymers

journal homepage: www.elsevier.com/locate/carbpol

Cross-linkage effect of cellulose/laponite hybrids in aqueous dispersions and solid films

Zaiwu Yuan[a,b], Qingrui Fan[b], Xiaonan Dai[b], Chao Zhao[b], Aijie Lv[b], Jingjing Zhang[b], Guiying Xu[a,*], Menghua Qin[b,c,**]

[a] Key Laboratory of Colloid and Interface Chemistry, Ministry of Education, Shandong University, Jinan 250100, China
[b] Key Laboratory of Pulp and Paper Science and Technology, Ministry of Education, Key Laboratory of Fine Chemicals in Universities of Shandong, Qilu University of Technology, Jinan 250353, China
[c] Laboratory of Organic Chemistry, Taishan University, Taian 271021, China

ARTICLE INFO

Article history:
Received 29 September 2013
Received in revised form 24 October 2013
Accepted 27 November 2013
Available online 5 December 2013

Keywords:
Cellulose aqueous solutions
Laponite
Composite film
Cross-linkage
Reinforcement

ABSTRACT

Homogenous cellulose/laponite aqueous dispersions and composite films were respectively prepared from the pre-cooling NaOH/urea aqueous systems. Rheological measurements of aqueous dispersions demonstrated a sol-to-gel transition triggered by loading of laponite, reflecting a cross-linkage effect of cellulose/laponite hybrids. Similarly, based on scanning electron microscopy (SEM), Fourier-transform infrared (FTIR) spectroscopy, and X-ray diffraction (XRD) characterizations, as well as mechanical and thermal measurements, the cross-linkage effect of cellulose/laponite hybrids was also found in solid films, which played an important role in improving the tensile strength (σ_b) of composite films. For instance, the σ_b exhibited a largest enhancement up to 75.7% at a critical laponite content of 0.100 wt%, indicating that the property of composite film was closely related with the dispersion and interaction state of laponite, i.e. its content in cellulose matrix. These results were expected to provide significant information for fabrication and utility of cellulose-based materials.

1. Introduction

Cellulose, as a kind of biodegradable material, has attracted great industrial and academic interest for sustainable development and environmental conservation because of its abundance, low cost, eco-friendly characteristics, and great potential to replace petrochemically derived compounds in many cases (Chen & Zhang, 2006; Cranston & Gray, 2006; Klemm, Heublein, Fink, & Bohn, 2005; Ma, Burger, Hsiao, & Chu, 2011). Generally, there are two obstacles for sufficient utility of cellulose. First, cellulose is difficult to process in solution or as a melt because of its large proportion of intra- and inter-molecular hydrogen bonds, which brings about large difficulties for fabrication of fiber-, film-, and bulk-based cellulose materials by regeneration method. Therefore, a variety of systems have been exploited and found for dissolution of cellulose. Among these systems including N,N-dimethylacetamide (DMAc)/LiCl (Kondo, Togawa, & Brown, 2001), N-methylmorpholine N-oxide (NMMO)/water (Fink, Weigel, Purz, & Ganster, 2001; Kulpinski, 2005), ionic liquid (Wu, Wang, Li, Li, & Wang, 2009; Zhao et al., 2007), etc., the pre-cooling NaOH/urea aqueous system (Cai & Zhang, 2006; Fukuzumi, Saito, Iwata, Kumamoto, & Isogai, 2008; Li et al., 2010) has attracted most attention because of its high efficiency, low cost, environmental friendliness, and facile procedure. This system, only cheap chemicals of NaOH and urea were used, offered a green and versatile means for machining of cellulose-based materials, which has greatly pushed forward the research process of cellulose-based material field.

Second, the pure cellulose materials usually possess poor mechanical and thermal properties and hence greatly hinder their practical applications. The inclusion of nanometer-scale fillers, such as montmorillonite (Cerruti et al., 2008; Mahmoudian, Wahit, Ismail, & Yussuf, 2012), carbon black (Knite, Teteris, Kiploka, & Kaupuzs, 2004), carbon nanotubes (Cha, Kim, Arshad, Mo, & Hong, 2005; Qi, Liu, Gao, & Mäder, 2013; Zhan, Kuntz, Wan, & Mukherjee, 2003), cellulose nanocrystals or nanowhiskers (Habibi, Lucia, & Rojas, 2010), and graphene oxide (Wang, Lou, Wang, & Hao, 2012), into cellulose matrix has been a common way to resolve the above problem. Wang et al. dissolved microcrystalline cellulose (MCC) in an ionic liquid, 1-butyl-3-methylimidazolium chloride ([Bmim]Cl), and then dispersed graphene oxide nanosheets in this solution, resulting in the reinforcement of the regenerated composite films (Wang et al., 2012). Cerruti et al. reported the preparation of cellulose/montmorillonite nanocomposites with high thermostability

* Corresponding author. Tel.: +86 531 88365436; fax: +86 531 88564750.
** Corresponding author at: Laboratory of Organic Chemistry, Taishan University, Taian 271021, China. Tel.: +86 538 6711009; fax: +86 538 6715521.
E-mail addresses: xuguiying@sdu.edu.cn (G. Xu), qmh@spu.edu.cn (M. Qin).

0144-8617/$ – see front matter © 2013 Elsevier Ltd. All rights reserved.
http://dx.doi.org/10.1016/j.carbpol.2013.11.051

by a precipitation method. Cellulose composite films were also prepared by blending native cellulose nanowhiskers in cellulose NaOH/urea aqueous solutions (Qi, Chang, & Zhang, 2009). Good comparability and strong interactions between the nanoadditives and cellulose matrix were considered to be the key factors for property performance of cellulose-based composite materials.

Laponite, synthetic layered silicate with high biocompatibility, is readily exfoliated into single two-dimensional (2D) thin nanoplatelets owing to the abundant oxygen-containing groups on its surfaces (Fig. S1). At a suitable concentration, the laponite could lead to gel formation in aqueous systems by electrostatic interactions between negatively charged faces and positively charged edges of the nanoplatelets, imparting these systems outstanding suspension, thixotropy and other unique properties. These features make laponite an ideal waterborne additive to improve the properties of a wide range of industrial products such as cosmetics, food, medicine, and paint (Mourchid & Levitz, 1998; Thompson & Butterworth, 1992; Willenbacher, 1996). However, it is a pity that few researches on cellulose-based materials using laponite as the nanoadditives have been reported.

In this work, laponite was dispersed into cellulose NaOH/urea aqueous solution to form aqueous dispersion. Then cellulose/laponite composite film was also obtained by regenerating from the aqueous dispersion. In order to reveal the dispersion and interaction state of cellulose/laponite hybrids in aqueous dispersions and solid films, rheological, mechanical, and thermal property measurements were conducted except for SEM, FTIR, and XRD characterizations. Meanwhile, based on the experimental results, the relationship between disperse and interaction state of cellulose/laponite hybrids and properties of the aqueous dispersions and composite films was proposed and discussed.

2. Experimental

2.1. Materials

Cellulose (cotton linter pulp) with a degree of polymerization (DP) of ~525 was supplied by Yinying Chemical Fiber Co. Ltd. (Gaomi, China). NaOH and urea were of analytical reagent grade (Shanghai Chemical Reagent Co. Ltd., China). Laponite with transmittance of over 99% was a gift from Huizhi Fine Chemical Co. Ltd. (Sihong, China). All of them were used as obtained without further purification.

2.2. Preparation of cellulose/laponite aqueous dispersions

An aqueous solution containing 7 wt% NaOH and 12 wt% urea was pre-cooled to −12 °C, into which a known amount of cellulose (4 wt%) was added and dispersed at a temperature between 0 and 4 °C under stirring. Then the 4 wt% cellulose solution was obtained after degassed by centrifugation at 4000 rpm for 5 min.

Laponite was first dispersed into pure water. Then a known weight of NaOH (7 wt%) and urea (12 wt%) was added under stirring for 30 min at 3000 rpm. Finally, a well dispersed suspension of laponite was obtained.

The two NaOH/urea aqueous systems, containing dissolved cellulose and dispersed laponite, respectively, were completely mixed by stirring, resulting in homogeneous and translucent cellulose/laponite aqueous dispersions with a fixed cellulose concentration (2 wt%) but different contents of laponite ($w_{laponite}$ = 0, 0.033, 0.067, 0.100, 0.133, and 0.167 wt%, respectively). It is worth noting that the dispersion with higher loading of laponite was not prepared because it became apparently turbid when the laponite content is above 0.167 wt%.

2.3. Preparation of cellulose/laponite composite films

The preparation procedures of cellulose/laponite composite films are shown in Fig. S2. Typically, the mold was first coated with a cellulose/laponite aqueous dispersion. Then, a wet film was regenerated by an acetone/water mixed solvent as coagulant and rinsed with pure water to remove NaOH and urea. Finally, the dry cellulose/laponite composite film was gained by a drying process in an oven for 24 h at a constant temperature (30 °C) and humidity (65%). Here, the adopted volume ratio of acetone to water was 2:1, at which the regenerated films were proved to possess best homogeneity. The as-produced cellulose/laponite composite films were named as F-0, 0.033, 0.067, 0.100, 0.133, 0.167 based on different weight fraction ($w_{laponite}$).

2.4. Rheological experiments

Rheological experiments of cellulose/laponite aqueous dispersions were carried out on a Haake RS6000 rheometer (Germany) with a coaxial cylinder sensor system (Z41 Ti) at different temperatures. The diameters of the rotor and the shear cell are 41.420 and 43.400 mm, respectively. An oscillation amplitude sweep at a fixed frequency of 1 Hz was performed prior to the following oscillation frequency sweep in order to ensure the selected stress was within the linear viscoelastic region of the samples. The samples were allowed to equilibrate in the shear cell for 5 min before each measurement.

2.5. Tensile strength measurements

The mechanical strength of the composite films, with a dimension of 0.4 cm × 5 cm and a thickness of 38–40 μm, was measured using an universal testing machine (Jinan Tianchen Testing Machine Manufacturing Co. Ltd., China) at a crosshead speed of 1 mm min^{-1} and a gauge length of 2 cm. At least five specimens were measured for each type of film to ensure the accuracy and reproducibility.

2.6. Other characterizations

The morphologies of the cellulose/laponite composite films were examined by scanning electron microscopy (SEM, JEOL JMS-6700) observation. The composite films were fractured in liquid nitrogen before gold was sputtered for the subsequent SEM observations. Fourier-transform infrared spectroscopy (FTIR) measurements were recorded on a Nexus 670 infrared spectrometer (Thermo-nicolet electron corporation, USA) using a KBr-disk method. X-ray diffraction (XRD) measurements were carried out with an X-ray diffractometer using a Cu Kα target at 40 kV and 30 mA. In FTIR and XRD measurements, the cellulose/laponite composite films were crushed into powders. Thermogravimetric analysis (TGA) was carried out on a TGA/SDTA851^e system (Mettler-Toledo, Swiss). The temperature was increased from 40 °C to 700 °C at a rate of 10 °C min^{-1} under nitrogen protection.

3. Results and discussion

3.1. Rheological properties of cellulose/laponite aqueous dispersions

Rheological measurement is one of the most promising means to reveal the characteristics of functional fluids, from which the microstructure of a fluid matrix could be inferred. Fig. 1 shows the elastic modulus (G') of the cellulose/laponite aqueous dispersions as a function of oscillation frequency at various temperatures. The applied shear stress was 0.04 Pa, which has been proved to

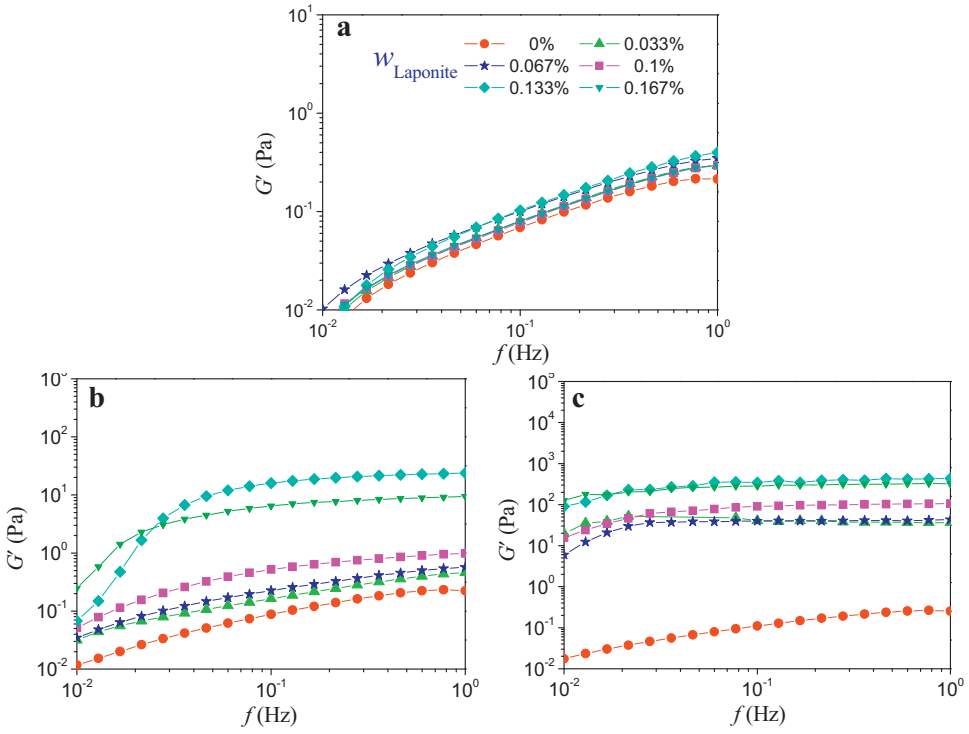

Fig. 1. Elastic modulus G' of the cellulose/laponite aqueous dispersions with different contents of laponite ($w_{laponite}$) as a function of oscillation frequency f at various temperatures of (a) 25, (b) 30, and (c) 35 °C, respectively.

be located within the linear viscoelastic region (Fig. S3). At a low temperature such as 25 °C (Fig. 1a), G' curves of all the tested aqueous dispersions scale with f ($G' \sim f$) with a slope of approximately 1 at low frequency, demonstrating typical liquid-like behaviors. Moreover, all the G' curves tend to overlap, illustrating that the addition of laponite exhibits slight effects on the viscoelastic properties of the cellulose aqueous dispersions at low temperature of 25 °C. On the other hand, these phenomena also reflect that the cellulose molecules and laponite nanoplatelets are well dispersed and compatible in 7 wt% NaOH/12 wt% urea solutions, which is of key importance for fabrication of regenerated cellulose-based materials.

When the temperature increases to 30 °C (Fig. 1b), the G' curves have different shapes and the G' values begin to display an obvious $w_{laponite}$-dependent behavior during the tested f range. Specifically, in the case of $w_{laponite} \leq 0.067$ wt%, the G' curves still characterize as upward sloping against f. While at high $w_{laponite}$ (>0.067 wt%), a plateau region appears in G' curve at high f. In addition, the higher the $w_{laponite}$, the larger will be the plateau region. All these features manifest a liquid-like to gel-like rheological property transition with the increment of laponite loading at 30 °C. As the temperature further increases to 35 °C (Fig. 1c), the G' values of cellulose/laponite aqueous dispersions are at least two orders of magnitudes higher that of pure cellulose system. Moreover, large plateau regions for G' curves could be observed even at a $w_{laponite}$ as low as 0.033 wt%, reflecting a remarkable gel-like behavior. Based on above description, several interesting opinions can be given. First of all, both the temperature and $w_{laponite}$ play important roles in the rheological behavior variation of cellulose/laponite aqueous dispersions. At low temperature of 25 °C, the interactions between cellulose molecules and laponite are weak owing to the hydration of hydroxyl groups in cellulose molecule. Hence, the loading of laponite has light effects on the viscoelastic properties of the cellulose aqueous dispersions. With increase of temperature to 30 °C, the situation changed. It is believed that raising temperature is instrumental for the dehydration of the hydroxyl groups on cellulose. So these released hydroxyl groups can then associate with the hydroxyl groups on laponite through hydrogen bonds. A three-dimensional network structure among laponite and cellulose could form with increase of laponite loading by cross-linkage effect of cellulose/laponite hybrids, which induces the sol-to-gel transition. In addition, no apparent changes in G' curves were found for the pure cellulose aqueous system ($w_{laponite} = 0$) with increasing temperature, indicating that the sol-to-gel transition occurred non-predominately from the H-bonding interactions among cellulose, but primarily from the H-bonding interactions between laponite and cellulose. When the temperature is 35 °C, this trend is further strengthened. The sol-to-gel transition was found even at $w_{laponite}$ as low as 0.033 wt%, reflecting the ultra-strong interactions between laponite and cellulose.

The cross-linkage effect of laponite in cellulose matrix can be found from the comparison between G' and the viscous modulus (G'') as a function of oscillation frequency f. For comparison, the results of a cellulose aqueous solution (2 wt%) and a laponite aqueous solution (0.100 wt%) are also given. It can be seen that the 0.100 wt% laponite aqueous solution is a typical viscous solution with G'' higher than G' over the whole frequency range (curves i), exhibiting distinctive liquid properties (Steffe, 1996). The same features can also be observed for 2 wt% cellulose aqueous solution (curves ii). However, G' begins to exceed G'' for 2 wt% cellulose/0.100 wt% laponite aqueous dispersions, directly exhibiting a typical gel-like behavior. Furthermore, this sol-to-gel transition tendency becomes more obvious with increase of laponite loading (Fig. S4).

The interactions between laponite and cellulose matrix was also evaluated by rheological experiments using a steady shear mode except for above oscillation mode (Fig. 2b). At 30 °C, the shear stresses (τ) for cellulose/laponite aqueous dispersions exhibit abundant variations with increase of laponite content. In the case of $w_{laponite} < 0.100$ wt%, the τ curves of cellulose/laponite aqueous dispersions are almost coincident with that of cellulose aqueous solution during tested $\dot{\gamma}$. At $w_{laponite} = 0.100$ wt%, the τ curve of

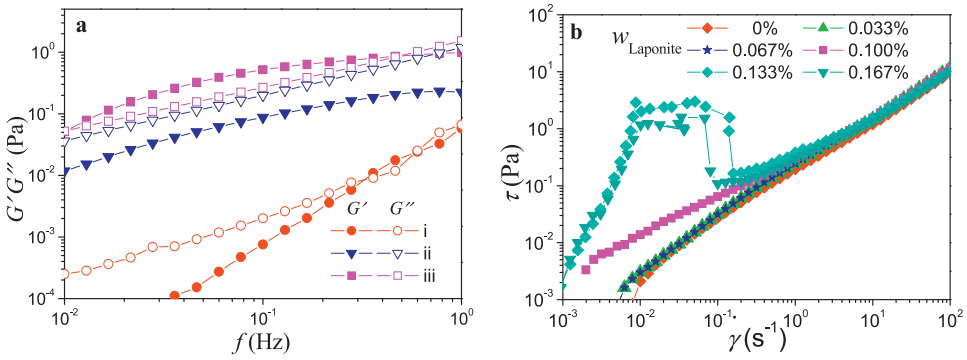

Fig. 2. (a) Elastic modulus G' and viscous modulus G'' as a function of oscillation frequency f at $T = 30\,^{\circ}C$ for (i) 0.100 wt% laponite, (ii) 2 wt% cellulose and (iii) 2 wt% cellulose/0.100 wt% laponite aqueous dispersion, and (b) shear stress (τ) curves for the cellulose/laponite aqueous dispersions with different $w_{laponite}$ at $T = 30\,^{\circ}C$.

dispersion is apparent higher than that of cellulose aqueous solution at low $\dot{\gamma}$ but nearly overlays each other at high $\dot{\gamma}$, indicating that the weak three-dimensional network structure formed by the cross-linkage effect is destroyed after the τ is inputted. While when the $w_{laponite} > 0.100$ wt%, in sharp contrast with that of cellulose aqueous solution, the τ of aqueous dispersions display a complicated transformation. As the $\dot{\gamma}$ increases, the τ first sharply rises, then fiercely falls after a plateau region, finally increases again and almost overlaps with that of cellulose aqueous solution. All the features demonstrate a shear destruction process of strong three-dimensional network structure, which agrees well with the results of oscillation shear mode. Based on the rheological experiments, we can conclude that below 30 °C is necessary to prepare the cellulose/laponite aqueous dispersions because the strong interactions between cellulose and laponite need to be avoided before their homogeneous blend.

3.2. Characterization of cellulose/laponite composite films

It was reported that the 5 wt% H_2SO_4/5 wt% Na_2SO_4 aqueous solution was a good coagulant to regenerate cellulose films or fibers (Mao, Zhang, Cai, Zhou, & Kondo, 2008; Zhang, Mao, Zhou, & Cai, 2005). Here, an acetone/water mixture solution was used as the coagulant to prepare the cellulose/laponite composite films because of the better reproducibility. In order to disclose dispersion and interaction state of laponite in cellulose matrix, relative characterizations were conducted.

Fig. 3 shows the typical SEM images of cross sectionals of the composite films with varying contents of laponite. Pure cellulose film (F-0) exhibits a comparatively loose structure with many large-size pores (Fig. 3a). With increase of laponite loading, the structures of films (F-0.067 and F-0.100) become denser and denser until small laponite clusters begin to appear (Fig. 3b and c). When the

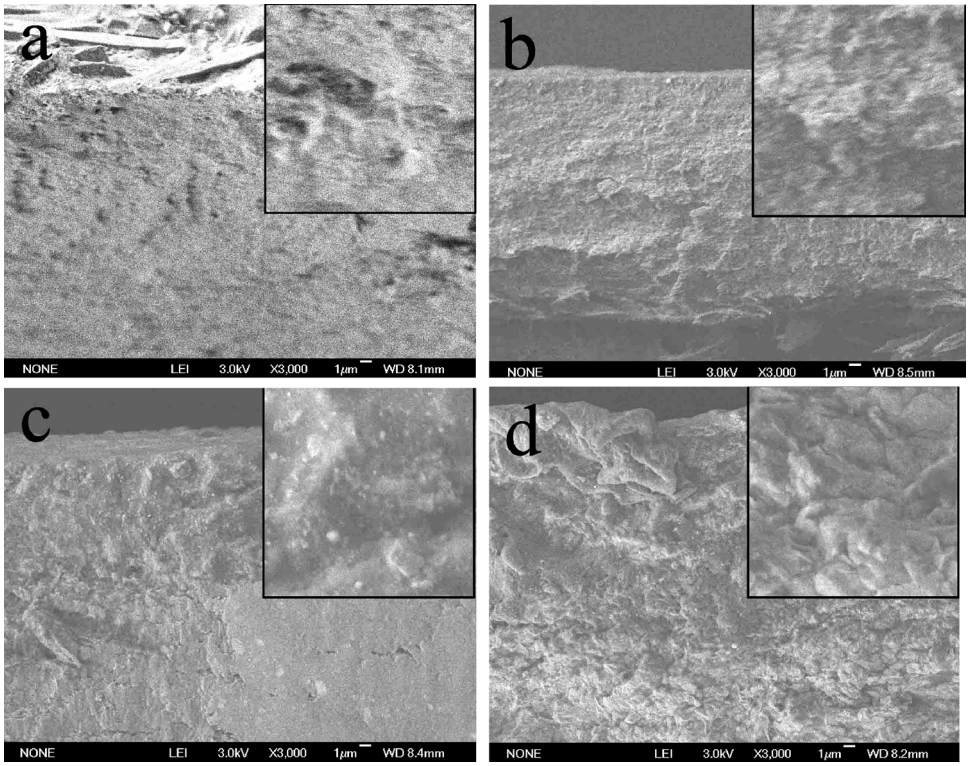

Fig. 3. Typical SEM images of the cross-sections of cellulose/laponite composite films of (a) F-0, (b) F-0.067, (c) F-0.100, and (d) F-0.167. The insets are their partially enlarged images.

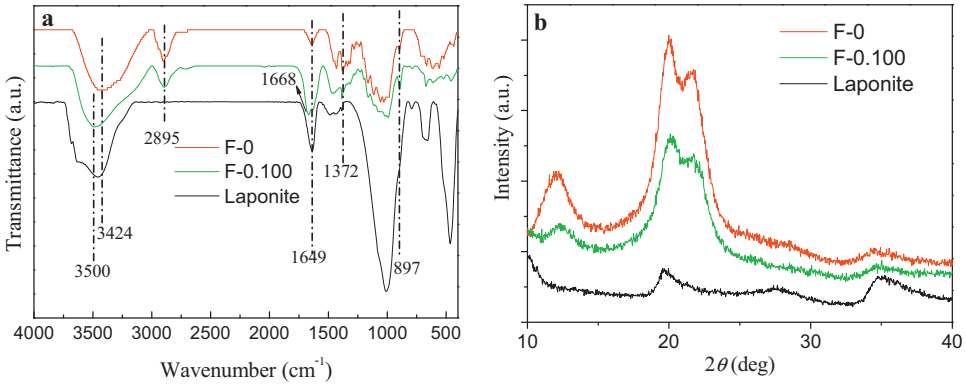

Fig. 4. FTIR (a) and XRD (b) spectra of pure cellulose film F-0, cellulose/laponite composite film F-0.100, and laponite powders.

laponite content further increases to 0.167 wt%, the structure of film (F-0.167) becomes loose again owing to formation of big laponite clusters (Fig. 3d). The morphology variations for cross sectionals of composite films illustrate homogeneous-to-aggregate dispersion and interaction state transition for laponite with the increase of laponite content.

The FTIR spectra of two representative films of F-0 and F-0.100, as well as the laponite powders, are shown in Fig. 4a. The absorption peaks at 2895 and 1372 cm^{-1} in both films are assigned to C—H stretching and bending vibrations, respectively. The peak at 897 cm^{-1} is corresponding to the C—O—C stretching vibrations of β-(1 → 4)-glycosidic linkages. In comparison with that of film F-0, the absorption band at 897 cm^{-1} for film F-0.100 is markedly enhanced, demonstrating that the crystallinity degree of cellulose film greatly reduces after introduction of laponite because this band is known as an "amorphous band". Similarly, the absorption peak at 1649 cm^{-1} for film F-0.100, associated with intramolecular hydrogen bonds, is greatly enhanced compared to that for film F-0. This feature means that strong H-bonding interactions are existent among cellulose molecules and laponite nanoplatelets. In addition, the blue shift of stretch vibrations of —OH groups in the range 3300–3500 cm^{-1} for film F-0.100 further verifies the existence of above hydrogen bond interactions. FTIR spectrum changes induced by laponite also reflect that the laponite nanoplatelets have good dispersibility and compatibility in cellulose matrix.

Fig. 4b shows the XRD spectra of films F-0 and F-0.100, as well as the laponite powders. Typical diffraction peaks for crystalline form of cellulose II at 21.6° (2 0 0), 19.9° (1 1 0), and 12.0° (1 $\bar{1}$ 0) are found in the spectra of both pure cellulose film and cellulose/laponite composite film F-0.100. While the diffraction peaks of laponite powders are not clearly observed in spectrum of composite film F-0.100, indicating that low amount of laponite have been completely exfoliated into cellulose matrix. It is also worth noting that the intensities of the diffraction peaks for film F-0.100 are much weaker than those for film F-0. This peak attenuation phenomenon could be attributed to the reduction of crystallinity degree of cellulose triggered by loading of laponite, which is consistent with the results of FTIR.

3.3. Mechanical and thermal properties of cellulose/laponite composite films

In order to further reveal the dispersion and interaction state between laponite and cellulose in solid films, the mechanical and thermal properties of the solid films were analyzed by mechanical property and TGA measurements, respectively. Stress–strain curves of the cellulose/laponite composite films with varying laponite contents are shown in Fig. 5a. As a whole, the mechanical strength of the composite films is closely linked with the content of laponite. At a critical content of 0.100 wt%, the tensile strength (σ_b) increases from 37 to 65 MPa, i.e. an enhancement up to 75.7%, which is considered to be a result of the cross-linkage effect of cellulose/laponite hybrids by intermolecular hydrogen bonds. In the contrary, the σ_b of composite films is obviously weaker than that of pure cellulose film when the content of laponite is 0.167 wt%. The above sharp contrast implies that the dispersion and interaction state of laponite in cellulose matrix is tightly related with the σ_b of composite films. In addition, the toughness (strain-to-failure) of composite films is moderately reduced in the tested laponite content range compared to that of pure cellulose film, which could be attributed to the decrease of crystallinity degree of cellulose caused by insertion of laponite nanoplatelets.

Fig. 5b displays the TGA curves of cellulose/laponite composite films with various contents of laponite. Although laponite is very stable in the tested temperature range, the decomposition temperatures of the composite films are greatly advanced from 330 to

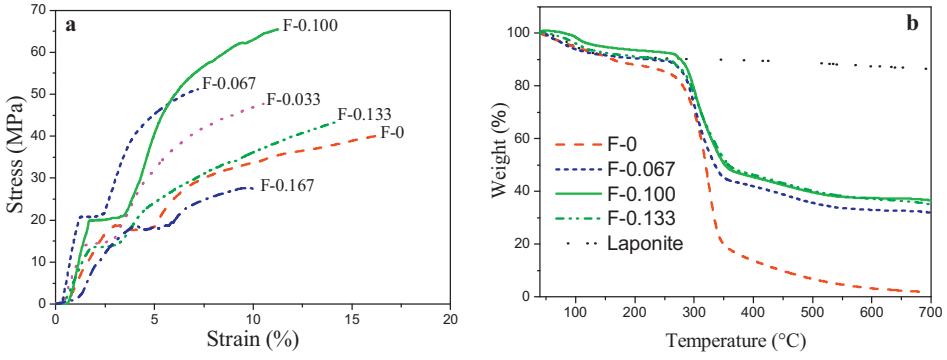

Fig. 5. (a) Stress–strain and (b) TGA curves of cellulose/laponite composite films with various contents of laponite.

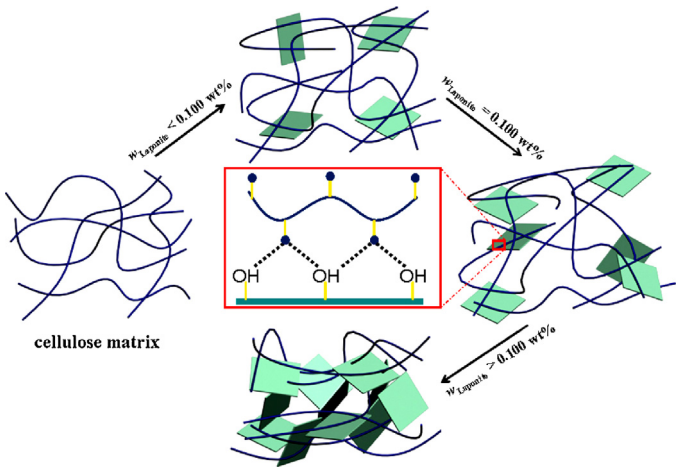

Scheme 1. Schematic illustration of dispersion and interaction state evolution of laponite in the cellulose/laponite composite films with increase content of laponite.

260 °C owing to introduction of laponite. Commonly, it was considered that the inorganic laponite could catalyze the decomposition of cellulose and hence result in decrease of its decomposition temperature (Zeng, Li, Liu, & Zhang, 2011; Zhou et al., 2009). We deduce that the decrease of crystallinity degree of cellulose in composite films may be another reason.

3.4. Relationship between dispersion and interaction state of laponite and property of composite films

The SEM images exhibit that moderate contents of laponite endow composite films with denser pack. While excess contents of laponite will form clusters in cellulose and loosen the pack of composite films. Both of FTIR and XRD spectra demonstrate that introduction of laponite makes the crystallinity degree of cellulose in composite films reduced. In addition, the FTIR also reflect that the laponite nanoplatelets have strong interactions with cellulose molecules by intermolecular hydrogen bonds. Based on above characterization results, Scheme 1 gives schematic representation which shows dispersion and interaction state evolution of laponite in the composite films with increase content of laponite. When the loading contents of laponite are comparatively low (below 0.100 wt%), laponite nanoplatelets can be homo-dispersed into cellulose matrix and play the role of a binding node to connect neighboring cellulose molecules by intermolecular hydrogen bonds, resulting in a cross-linkage effect and hence reinforces the tensile strength of composite films. As the content increases to a critical content of 0.100 wt%, the cross-linkage effect expresses the greatest efficiency and a largest σ_b enhancement up to 75.7% is gained. If the content further increases, laponite clusters in cellulose matrix begin to appear. The "house of cards" structure remarkably damages the homogeneity of composite films, leading to decrease of mechanical property of composite films. Once the content is too high, the σ_b of the composite films is even lower than that of pure cellulose film. On the other hand, no matter how laponite nanoplatelets disperse in cellulose matrix, the decrease of crystallinity degree of cellulose in composite films is inevitable. Hence, the toughness and decomposition temperature of composite films are markedly declined compared to those of pure cellulose film.

4. Conclusions

In summary, the cellulose/laponite aqueous dispersions and composite films were respectively prepared by a green pre-cooling NaOH/urea aqueous system. Rheological measurements of cellulose/laponite aqueous dispersions illustrated an interesting sol-to-gel transition with increase of laponite loading. Adding 0.100 wt% of laponite into cellulose matrix brought about a tremendous σ_b enhancement up to 75.7%. These rheological behavior variations in aqueous dispersions and reinforce effects in composite films both reflected the cross-linkage effect of cellulose/laponite hybrids by intermolecular hydrogen bonds. However, the toughness and thermal property of composite films were obviously reduced because the introduction of laponite resulted in the decrease of crystallinity degree of films. Moreover, given the results of performance tests and structure characterizations, the closely connected relationship between dispersion and interaction state of laponite in cellulose matrix and property of composite films was deduced, which was expected to provide significantly experimental and theoretical guidance for fabrication and utility of cellulose-based materials.

Acknowledgements

This work was supported by the China Postdoctoral Science Foundation (2012M511491), Shandong Province Young and Middle-Aged Scientists Research Awards Fund (BS2012CL030), and the Program for the Scholar of Yellow River Mouth (DYRC20120105). The authors would like to thank Dr. Renhao Dong for SEM observation and Dr. Baogang Wang for helpful discussion.

Appendix A. Supplementary data

Supplementary data associated with this article can be found, in the online version, at http://dx.doi.org/10.1016/j.carbpol.2013.11.051.

References

Cai, J., & Zhang, L. (2006). Unique gelation behavior of cellulose in NaOH/urea aqueous solution. *Biomacromolecules*, *7*, 183–189.
Cerruti, P., Ambrogi, V., Postiglione, A., Rychlý, J., Matisová-Rychlá, L., & Carfagna, C. (2008). Morphological and thermal properties of cellulose–montmorillonite nanocomposites. *Biomacromolecules*, *9*, 3004–3013.
Cha, S. I., Kim, K. T., Arshad, S. N., Mo, C. B., & Hong, S. H. (2005). Extraordinary strengthening effect of carbon nanotubes in metal–matrix nanocomposites processed by molecular-level mixing. *Advanced Materials*, *17*, 1377–1381.
Chen, P., & Zhang, L. (2006). Interaction and properties of highly exfoliated soy protein/montmorillonite nanocomposites. *Biomacromolecules*, *7*, 1700–1706.
Cranston, E., & Gray, D. (2006). Formation of cellulose-based electrostatic layer-by-layer films in a magnetic field. *Science and Technology of Advanced Materials*, *7*, 319–321.
Fink, H. P., Weigel, P., Purz, H., & Ganster, J. (2001). Structure formation of regenerated cellulose materials from NMMO-solutions. *Progress in Polymer Science*, *26*, 1473–1524.
Fukuzumi, H., Saito, T., Iwata, T., Kumamoto, Y., & Isogai, A. (2008). Transparent and high gas barrier films of cellulose nanofibers prepared by TEMPO-mediated oxidation. *Biomacromolecules*, *10*, 162–165.
Habibi, Y., Lucia, L. A., & Rojas, O. J. (2010). Cellulose nanocrystals: Chemistry, self-assembly, and applications. *Chemical Reviews*, *110*, 3479–3500.
Klemm, D., Heublein, B., Fink, H. P., & Bohn, A. (2005). Cellulose: Fascinating biopolymer and sustainable raw material. *Angewandte Chemie International Edition*, *44*, 3358–3393.
Knite, M., Teteris, V., Kiploka, A., & Kaupuzs, J. (2004). Polyisoprene–carbon black nanocomposites as tensile strain and pressure sensor materials. *Sensors and Actuators A: Physical*, *110*, 142–149.
Kondo, T., Togawa, E., & Brown, R. M., Jr. (2001). "Nematic ordered cellulose": A concept of glucan chain association. *Biomacromolecules*, *2*, 1324–1330.
Kulpinski, P. (2005). Cellulose nanofibers prepared by the N-methylmorpholine-N-oxide method. *Journal of Applied Polymer Science*, *98*, 1855–1859.
Li, R., Chang, C., Zhou, J., Zhang, L., Gu, W., Li, C., et al. (2010). Primarily industrialized trial of novel fibers spun from cellulose dope in NaOH/urea aqueous solution. *Industrial & Engineering Chemistry Research*, *49*, 11380–11384.
Ma, H., Burger, C., Hsiao, B. S., & Chu, B. (2011). Ultrafine polysaccharide nanofibrous membranes for water purification. *Biomacromolecules*, *12*, 970–976.
Mahmoudian, S., Wahit, M. U., Ismail, A., & Yussuf, A. (2012). Preparation of regenerated cellulose/montmorillonite nanocomposite films via ionic liquids. *Carbohydrate Polymers*, *88*, 1251–1257.

Mao, Y., Zhang, L., Cai, J., Zhou, J., & Kondo, T. (2008). Effects of coagulation conditions on properties of multifilament fibers based on dissolution of cellulose in NaOH/urea aqueous solution. *Industrial & Engineering Chemistry Research*, *47*, 8676–8683.

Mourchid, A., & Levitz, P. (1998). Long-term gelation of laponite aqueous dispersions. *Physical Review E*, *57*, 4887–4890.

Qi, H., Chang, C., & Zhang, L. (2009). Properties and applications of biodegradable transparent and photoluminescent cellulose films prepared via a green process. *Green Chemistry*, *11*, 177–184.

Qi, H., Liu, J., Gao, S., & Mäder, E. (2013). Multifunctional films composed of carbon nanotubes and cellulose regenerated from alkaline-urea solution. *Journal of Materials Chemistry A*, *1*, 2161–2168.

Steffe, J. F. (1996). *Rheological methods in food process engineering*. East Lansing: Freeman Press.

Thompson, D. W., & Butterworth, J. T. (1992). The nature of laponite and its aqueous dispersions. *Journal of Colloid and Interface Science*, *151*, 236–243.

Wang, B., Lou, W., Wang, X., & Hao, J. (2012). Relationship between disperse state and reinforcement effect of graphene oxide in microcrystalline cellulose/graphene oxide composite films regenerated from microcrystalline cellulose/1-butyl-3-methylimidazolium chloride solutions. *Journal of Materials Chemistry*, *22*, 12859–12866.

Willenbacher, N. (1996). Unusual thixotropic properties of aqueous dispersions of laponite RD. *Journal of Colloid and Interface Science*, *182*, 501–510.

Wu, R. L., Wang, X. L., Li, F., Li, H. Z., & Wang, Y. Z. (2009). Green composite films prepared from cellulose, starch and lignin in room-temperature ionic liquid. *Bioresource Technology*, *100*, 2569–2574.

Zeng, J., Li, R., Liu, S., & Zhang, L. (2011). Fiber-like TiO_2 nanomaterials with different crystallinity phases fabricated via a green pathway. *ACS Applied Materials & Interfaces*, *3*, 2074–2079.

Zhan, G.-D., Kuntz, J. D., Wan, J., & Mukherjee, A. K. (2003). Single-wall carbon nanotubes as attractive toughening agents in alumina-based nanocomposites. *Nature Materials*, *2*, 38–42.

Zhang, L., Mao, Y., Zhou, J., & Cai, J. (2005). Effects of coagulation conditions on the properties of regenerated cellulose films prepared in NaOH/urea aqueous solution. *Industrial & Engineering Chemistry Research*, *44*, 522–529.

Zhao, H., Kwak, J. H., Wang, Y., Franz, J. A., White, J. M., & Holladay, J. E. (2007). Interactions between cellulose and N-methylmorpholine-N-oxide. *Carbohydrate Polymers*, *67*, 97–103.

Zhou, J., Li, R., Liu, S., Li, Q., Zhang, L., Zhang, L., et al. (2009). Structure and magnetic properties of regenerated cellulose/Fe_3O_4 nanocomposite films. *Journal of Applied Polymer Science*, *111*, 2477–2484.